



FIELD OBSERVATION OF SEAWATER SPRAY DROPLETS IMPINGING ON THE UPPER DECK OF AN ICEBREAKER

Toshihiro Ozeki ¹, Genki Sagawa ²

¹Hokkaido University of Education, Sapporo, JAPAN

²Weathernews Inc. JAPAN

ABSTRACT

Seawater spray icing is a major problem faced not only by fishing vessels and trawlers but also by commercial vessels. Marine disasters caused by ice accretion occur frequently in cold regions. However, even today, deicing continues to be a manual operation that usually involves the use of a hammer.

To address icing on the ship, sea spray generation, spray delivery, and heat transfer for ice accretion are important. In this study, we developed a seawater droplet counter for measuring the droplets impinging on ships.

The field observation was made on the upper deck of the CCGS Louis S. St-Laurent during the voyage to the Northwest Passage and the Canada Basin. Because the observation period was late July and August of 2012, the purpose of this observation was to obtain the relationship between pitching and rolling of the ship and seawater spray generation. The weather conditions, acceleration of the ship, and size and number of seawater droplets were measured. The marine condition and spray generation were recorded by using a monitoring system set up on the upper deck of the ship.

Droplet size distributions were obtained in rough weather. Preliminary result shows that long-period swells did not contribute to the increase in the amount of seawater spray, although the pitching angle of the ship increased with swell. The seawater droplet counter recorded large numbers of particles during a storm. The time series of the droplet counter suggested that the particles were caused by raindrops, because droplets were detected continuously.

INTRODUCTION

Seawater spray icing is a major problem faced by ships and offshore structures. Marine disasters caused by ice accretion occur frequently around Newfoundland and Nova Scotia (Kubat and Timco, 2005), and around Kuril Islands (Ono, 1974). Ice accretion is a substantial challenge for fishing vessels, trawlers, patrol boats, and commercial vessels.

In recent years, the summer condition of the Arctic Ocean has been changing each year and will undergo further changes as global warming progresses. Expansion of the open water area on the Northern Sea Route and the Northwest Passage increases the frequency of sea spray generation. Because the air temperature remains cold enough, conditions are suitable for sea spray icing. Heavy sea spray icing on ships affects the need for maintenance while navigating the cold regions. However, currently, removal of ice continues to be a manual operation involving the use of a hammer.

Rapid growth of ship icing occurs due to ice accretion by seawater spray. Ryerson and Gow (2000) studied the microstructural features of spray ice on ships and confirmed the existence of a channelized network of brine. Ozeki et al. (2005) designed a nuclear magnetic resonance imaging system to measure the three-dimensional microstructure of seawater spray ice. A channelized network of brine was confirmed in natural seawater spray ice samples. Lozowski

et al. (2000) reviewed computer simulations of marine ice accretion. The typical growth mechanism of sea spray icing is as follows: sea spray generation from the bow, drift and impingement of the spray to the superstructure, and wet growth of ice from brine water flow.

In this study, we developed a seawater droplet counter for measuring the droplets impinging on ships. The droplet counter can measure the particle size distribution every second. Thus, the flux distribution and the transport rate could be calculated as a function of particle size. The measurement of spray size distribution is useful for the study of mass flux and heat flux of ship

icing model. We investigated the drop size of seawater spray on the CCGS Louis S. St-Laurent (Figure 1).

This study is part of a research project entitled “Development of Ice Prediction and Navigation Assistant System for Utilization of the Northern Sea Route” of the GREEN program, Japan.

OBSERVATION METHODS AND INSTRUMENTS

Observation Route

In late July and August of 2012, field observations were conducted on the CCGS Icebreaker Louis S. St-Laurent. The vessel was conducting sea ice observation in the Northwest Passage and the Canada Basin (Figure 2). The observation period was late July and August of 2012, therefore the purpose of this observation was to obtain the relationship between pitching and rolling of the ship and seawater spray generation. The present study of sea spray drops was conducted during navigation from St. John's to the Lancaster Sound, and the Canada Basin. Because sea spray is generated on open water, the amount of sea spray was minimal during navigation in the Northwest Passage from the Lancaster Sound to the Canada Basin, which covered by sea ice.



Figure 1 Canadian Coast Guard Heavy Arctic Icebreaker, CCGS Louis S. St-Laurent (11,345 GRT) and location of SPC spray drop counter.

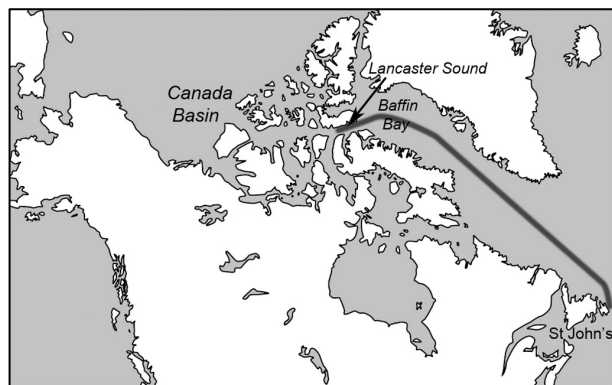


Figure 2 Observation Route. 1) between St. John's and Lancaster Sound. 2) Canada Basin.

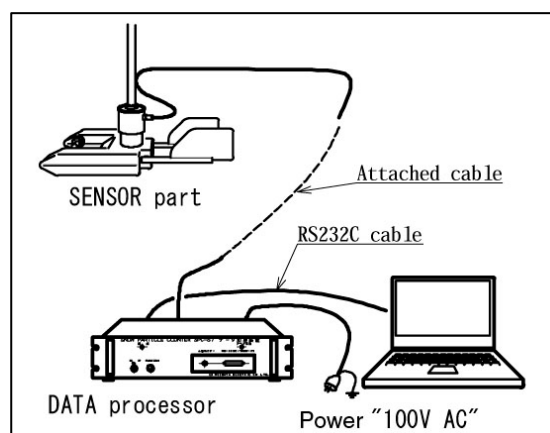


Figure 3 Schematic view of SPC spray drop counter.

Underway Data

The weather conditions and size and number of seawater droplets were measured. Wind velocity, air temperature, sea temperature, salinity, air pressure were provided by the CCGS Louis S. St-Laurent. Wind velocity may be related to sea spray generation and spray delivery. An interval camera system was set up by Kitami Institute of Technology on the upper deck. The camera monitored the front view during the voyage, and the recorded interval photographs provided the information of marine conditions (open water, melt pond, and sea ice). Movement of the ship was measured by the three-axis accelerometer to obtain pitching and rolling of the ship.

Sea-Spray Drop Counter

The size and number of seawater droplets were measured on the upper deck using a spray particle counter (SPC). The SPC was originally developed for measurement of drifting snow (Kimura et al, 1993). The SPC (SPC-S7; Niigata Denki) consists of a sensor, data processor, and personal computer (Figure 3). The sensing area was 25 mm wide, 2 mm high, and 0.5 mm deep, and SLD light is used as parallel ray. The sensor has a rudder to direct the sensing device toward the wind, and measures light attenuation by particle that pass through the sensing area. The processor distinguishes the particles into 32 classes depending on their diameters. The particle numbers in each class are measured every second. Thus the flux distribution and the transport rate could be calculated as a function of particle size (Nishimura and Nemoto, 2005).

The SPC for drifting snow divides the particles into 32 classes between 50–500 μm in diameter. It was tested using the spray nozzles, as we set up it on board. Figure 4

shows the size distribution of smaller droplets spray nozzle (VE115-31, Ikeuchi: spray angle 115° , 2.5 l/min). Accumulated numbers for 7 minutes were indicated. The SPC detected comparatively smaller droplets, although the SPC could not detect particles smaller than 50 μm in diameter. The maximum range was 81 μm . The maximum range of water drop volume, which was calculated as the spherical equivalent, was 317 μm , because the small drops do not contribute much to the flux amount in general. Figure 5 shows the size distribution of larger droplets spray nozzle (VE115-59, Ikeuchi: spray angle 115° , 4.1 l/min). Accumulated

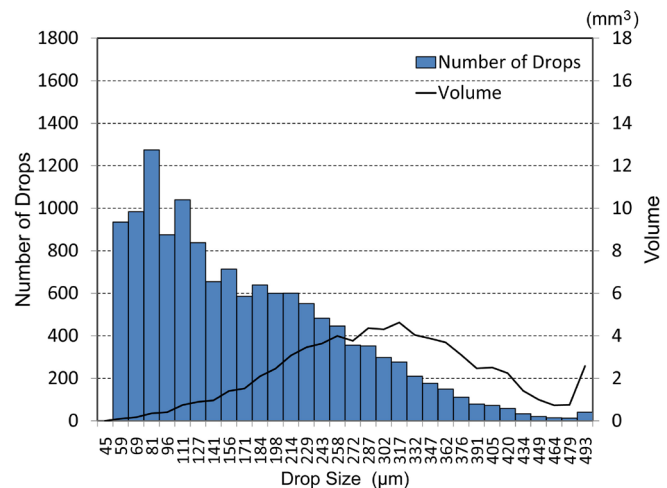


Figure 4 Size and flux distribution by smaller droplets spray nozzle. Total of 7 min.

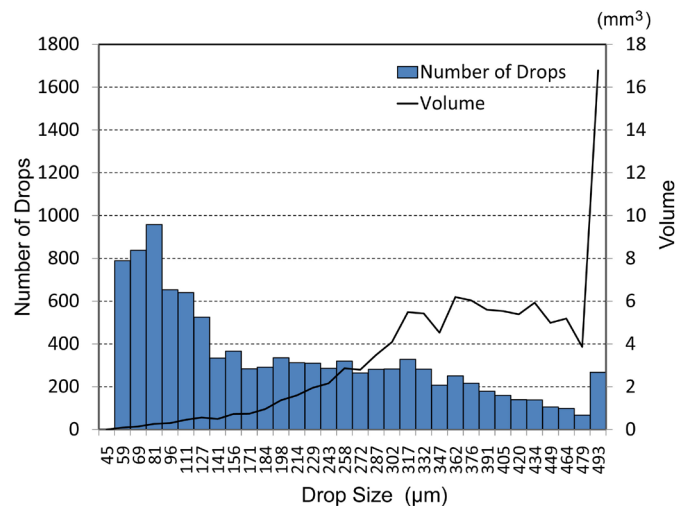


Figure 5 Size and flux distribution by larger droplets spray nozzle. Total of 8 min.

numbers for 8 minutes were indicated. The maximum range was 81 μm ; however there was a wide size distribution. Because large spray droplets increase the spray volume, the higher range of water drop volume was between 350–450 μm in diameter. The SPC detected particles larger than 500 μm , which were incorporated into the largest class (493 in Figure 5). According to the test result, 500 μm the maximum range was too small to measure the size distribution of VE115-59 nozzle. The consideration of these results, the measurement range of the SPC was improved to between 100–1000 μm (Ozeki, 2011). The SPC was set up in the front of the upper deck (Figure 1). The sensor has waterproof property, salinity tolerance and weatherability, therefore it is available to use on board. However, the sensor cannot be installed in an environment where green water impinging, because it has not been considered collision with large mass. The operating temperature of SPC is between $-20\text{ }^{\circ}\text{C}$ and $20\text{ }^{\circ}\text{C}$. On the other hand, anti-icing of the sensor is not enough under the heavy icing condition. The icing is necessary to remove from the sensor using the warm water by hand operation.

OBSERVATIONS

Observation on the Northwest Passage

The CCGS Louis S. St-Laurent sailed from St. John's on July 20. The voyage from St. John's to the Lancaster Sound was on open water, although icebergs were founded sometimes. Air temperature and sea temperature were almost above $0\text{ }^{\circ}\text{C}$. High pitching and rolling angles were recorded on July 21. Figure 6 shows the rolling and the pitching angles measured during the period 0 to 24 UTC on July 21. The average values for 10 minutes were indicated. Strong northwesterly wind more than 30 m/s was measured during the period from 01:00 to 02:00 UTC, and high pitching angle more than 6 degree were recorded.

The SPC was able to satisfactorily

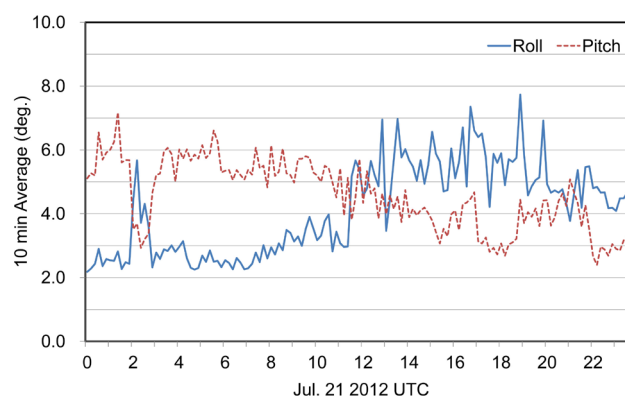


Figure 6 Rolling and pitching angles during the period from 0 to 24 UTC on July 21.

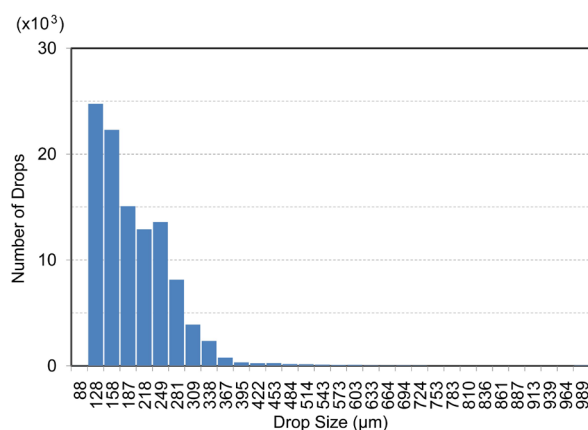


Figure 7 Spray drop size distribution during the period from 01:00 to 02:00 on July 21.

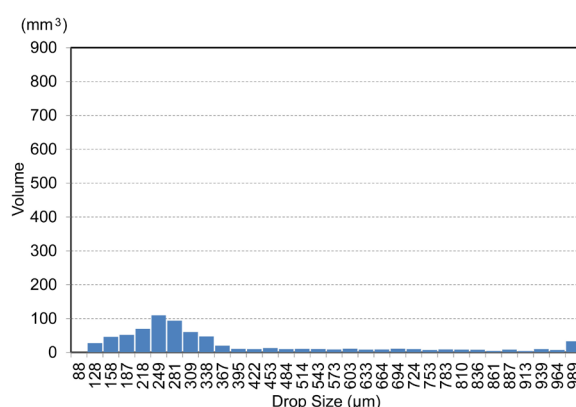


Figure 8 Spherical equivalent water drop volumes passing the gate of the SPC during the period from 01:00 to 02:00 on July 21.

perform measurements of the drops throughout the observation period. Figure 7 shows the size distribution of seawater spray droplets recorded on the upper deck during the period from 01:00 to 02:00 on July 21. The measurement interval was 1 s, and values were accumulated for 1 hour. The SPC detected comparatively smaller droplets during this period. The maximum range was 128 μm . Figure 8 shows the spherical equivalent water drop volumes passing the gate of the SPC during this period. Because large spray droplets increase the spray volume, the maximum range was 249 μm . In this period, the amount of seawater spray was recorded the maximum of the navigation through the Northwest Passage. However, the value was not large. On the other hand, high rolling angle was recorded in the afternoon of July 21. The maximum was around 19 UTC. It was owing to strong swells. As shown in Figure 9, the number of seawater spray droplets was not large in this period. It indicates that long-period swells did not contribute to the increase in the amount of seawater spray, although the pitching and rolling angles of the ship increased with swell. The seawater spray was not measured during navigation on the Northwest Passage from the Lancaster Sound to Kugluktuk, because this area was covered by sea ice.

Observation on the Canada Basin

The navigation of the Canada Basin was conducted on August of 2012. The underway data indicates that the route was covered with sea ice during first half of August. There were several times the opportunity to sail the open water in stormy weather in late August. Because the air temperature was almost 0 $^{\circ}\text{C}$, the sea spray icing was not observed.

The SPC detected a lot of seawater spray droplets during the period from 01:00 to 02:00 on August 28 UTC. The amount of sea spray in this period was the largest in the observation period. Figure 10 shows the spherical equivalent water drop volumes during the period. The seawater droplets were distributed widely: 100-300 μm droplets were the main range of volume. Additionally, the SPC has detected a lot of droplets larger than 500 μm which contributed to increase the spray volume. In this period, strong wind about 20 m/s was blowing from the side of the ship. Figure 11 shows the rolling and the pitching angles measured during the period from 12:00 on August 27 to 12:00 on August 28. The average values for 10 minutes were indicated. Both of rolling and pitching were smaller than 1 degree. It suggested that the detected particles were not related to the rolling and pitching of the ship in this period.

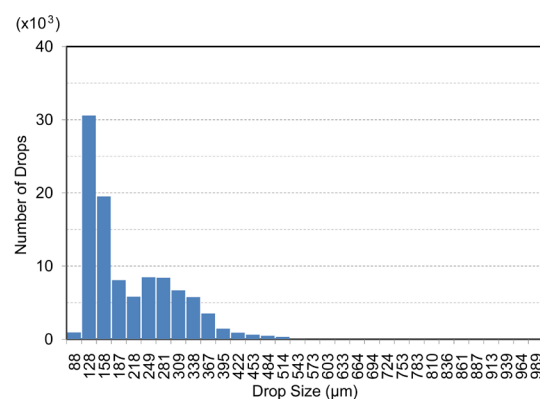


Figure 9 Spray drop size distribution during the period from 18:45 to 19:45 on July 21.

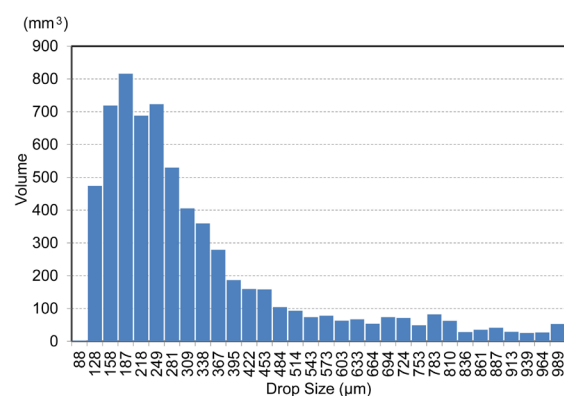


Figure 10 Spherical equivalent water drop volumes passing the gate of the SPC during the period from 01:00 to 02:00 on August 28.

The SPC responds to not only water droplets but also precipitation. The record during the storm might include rain drops and seawater spray. Figure 12 shows time series of number of drops during the period from 01:05 to 01:15 on August 28. On the other hand, Figure 13 shows number of drops during the period from 01:10 to 01:20 on July 21. The measuring interval of both figures was 1 s. Spikes of signal were observed in Figure 13. It indicates the seawater spray generated by ship. Droplets were detected continuously in Figure 12, although perturbation of signals was seen. It was suggested that the SPC detected raindrops during this period.

CONCLUSIONS

Field observations of seawater spray were conducted on the upper deck of the CCGS Louis S. St-Laurent during a voyage from St. John's to Lancaster Sound and Canada Basin in summer of 2012. In this study, we observed impinging seawater spray using SPC seawater droplet counter. The SPC was improved to divide the particles into 32 classes between 100–1000 μm in diameter. The SPC was able to satisfactorily perform measurements of the drops throughout the observation period. The transport distributions of droplets were calculated in several periods as a function of particle size. High pitching and rolling were recorded on July 21. The SPC detected a lot of seawater spray droplets in this period; however the value of water drop volume was not large. Long-period swells did not contribute to the increase in the amount of seawater spray in this case. On the other hand, SPC recorded the largest number of droplets during a storm on August 27 -28. The rolling and pitching angles were not large although the wind speed was about 20 m/s. Because the SPC responds to not only seawater droplets but also precipitation, we attempted to distinguish between precipitation and seawater spray. The time series of the particles on August 28 was compared with the record on July 21 using 1 s time resolution. It was suggested that the large number of droplets recorded on August 28 was caused by raindrops, because droplets were detected continuously. These were preliminary results of the SPC measurement. The detail of drop size distribution, flux, and the relation between impinging spray to ship motion are further investigations.

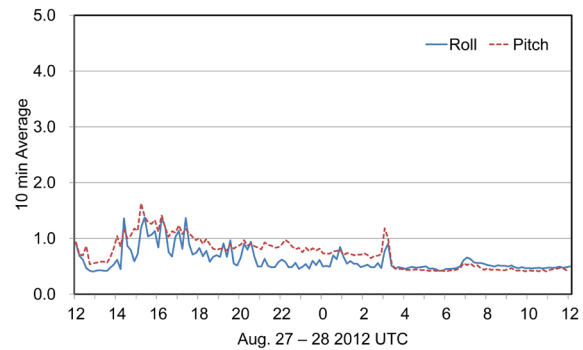


Figure 11 Rolling and pitching angles during the period from 0 to 24 UTC on July 21.

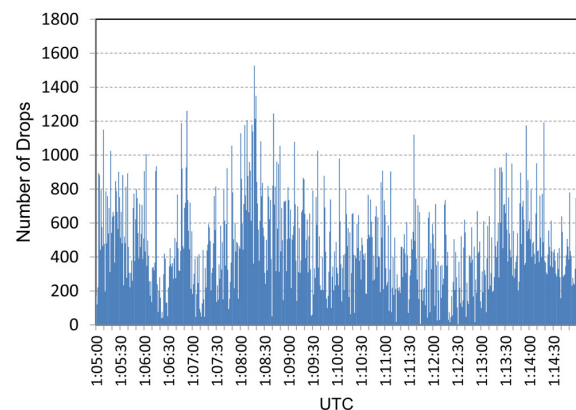


Figure 12 Number of drops during the period from 01:05 to 01:15 on August 28. Time series of every 1 s.

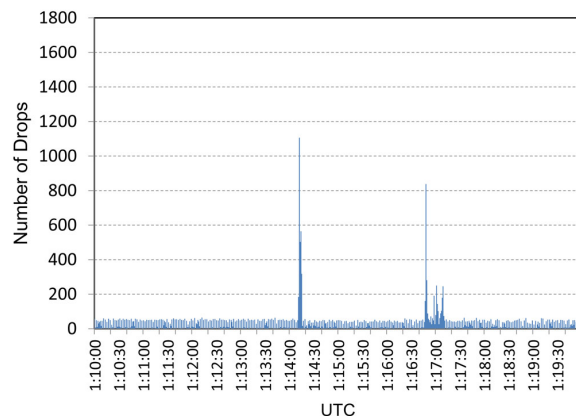


Figure 13 Number of drops during the period from 01:10 to 01:20 on July 21. Time series of every 1 s.

Acknowledgments

We wish to express our gratitude to Dr. H. Yamaguchi and Dr. J. Ono of University of Tokyo, Dr. K. Tateyama and Dr. H. Shibata of the Kitami Institute of Technology, and M. Yoshikawa of Weathernews Inc. for their support during field observations. We would like to thank the captain and crew of the CCGS Louis S. St-Laurent for their support on the ship. This research was supported by the research program of the Green Network of Excellence, MEXT, Japan.

REFERENCES

- Timoshenko, S. and Goodier, J. N., 1951. *Theory of Elasticity*. McGraw-Hill Book Company, Inc., 506 pp.
- Kubat, I. and Timco G., 2005. NRC Marine Icing Database. Proc. 11th Int. Workshop on Atmospheric Icing of Structures, Montreal, Que, 6 pp.
- Kimura, T., Maruyama, T. and Ishimaru, T., 1993. SPC-III no sekkei to seisaku. 9th Proc. Cold Region Technology Conference, 665–670. [in Japanese]
- Lozowski, E. P., Szilder, K., and Makkonen, L., 2000. Computer simulation of marine ice accretion. *Phil. Trans. R. Soc. Lond.*, A358, 2811–2845.
- Nishimura, K. and Nemoto, M., 2005. Blowing snow at Mizuho station, Antarctica. *Phil. Trans. R. Soc.*, A363, 1647–1662.
- Ono, N., Studies on the ice accumulation on ships. 2. On the conditions for the formation of ice and the rate of icing. *Low Temp. Sci.*, A22, 171–181 (1964). [in Japanese with English summary]
- N. Ono, 1964. Studies on ice accumulation on ships. 4. Statistical Analysis of Ship-Icing Condition. *Low Temp. Sci.*, A32, 235–242. [in Japanese with English summary]
- Ozeki, T., Kose, K., Haishi, T., Nakatsubo, S. and Matsuda, Y., 2005. Network images of drainage channels in sea spray icing by MR microscopy. *Mag. Res. Imag.*, 23, 333–335.
- Ozeki, T., 2011. Field investigations of sea spray droplets generated by icebreaker Shirase. 27th Proc. Cold Region Technology Conference, 5 pp. [in Japanese]
- Ozeki, T., Yamamoto, R., Izumiyama, K. and Sakamoto, T., 2012. Ice adhesion tests on pliable polymer sheets for protection against sea spray icing. *J. Adhesion Sci. Tech.*, 26, 651–663.
- Ryerson, C. C. and Gow, A. J., 2000. Crystalline structure and physical properties of ship superstructure spray ice. *Phil. Trans. R. Soc. Lond.*, A358, 2847–2871 (2000).